Study of the Optical Shubnikov-de Haas Effect*†

F. P. Missell‡§
Department of Physics, Massachusetts Institute of Technology, Cambridge, Massachusetts 02139

and

M. S. Dresselhaus§
Department of Electrical Engineering and Center for Materials Science and Engineering, Massachusetts Institute of Technology, Cambridge, Massachusetts 02139
and Lincoln Laboratory, Massachusetts Institute of Technology, Lexington, Massachusetts 02173

(Received 6 August 1971)

Studies of the dependence of the optical Shubnikov–de Haas effect on magnetic field, photon energy, and crystalline orientation have been carried out to determine the basic physical mechanisms involved in the observation of this effect in the reflectivity. For magnetic fields near 100 kG, fractional changes in the reflectivity, $[R(H)-R(0)]/R(0)$, as large as 100% have been observed, which can be associated with the passage of a Landau level through the Fermi surface. Furthermore, these large reflectivity oscillations are observed in the energy range $0.0670 \leq \hbar\omega \leq 0.3655$ eV, not just in the vicinity of the plasma edge (~ 0.117 eV) as previously reported, and the amplitudes of these reflectivity oscillations are found to be roughly independent of the photon energy. These observations appear to be inconsistent with the model used by Dresselhaus and Mavroides to interpret the reflectivity oscillations which they observed near the plasma edge. The identification of the present reflectivity oscillations with the optical Shubnikov–de Haas effect is based on the frequency independence of the resonant magnetic fields and on the excellent agreement with the periods measured in other de-Haas–van-Alphen–type experiments for the corresponding crystallographic orientations. To explain the large magnitudes of the reflectivity oscillations, a magnetic-field-dependent and oscillatory relaxation time is required. Furthermore, to explain the persistence of these oscillations for photon energies far above the plasma edge, it seems necessary to explicitly include the effects of interband transitions.

I. INTRODUCTION

The magnetic-energy-level structure of antimony has been studied extensively by experimental techniques which detect the passage of Landau levels through the Fermi surface. These include the de Haas–van Alphen (dHvA),[1–3] Shubnikov–de Haas (SdH),[4–6] ultrasonic attenuation,[7] magnetothermal,[8,9] and optical Shubnikov–de Haas[10] experiments. In the latter experiments, Dresselhaus and Mavroides (DM) observed a series of frequency-independent oscillations in the optical reflectivity which were found to be periodic in the inverse magnetic field, with periods which were in good agreement with the periods measured in other dHvA-like experiments for the corresponding crystallographic orientations. Their data were interpreted in terms of magnetic-field-dependent carrier-density oscillations in the high-frequency conductivity and this model was adequate for the explanation of most of their observations.

In this paper we will be concerned with optical SdH measurements made using a laser source, over a wide range of photon energies, at temperatures near the λ point of liquid He. Initially, these measurements were expected to constitute a detailed confirmation of the predictions of the model used by DM to interpret their experiments, especially with regard to the dependence of the line shape on magnetic field and photon energy and the dependence of the amplitudes of the reflectivity oscillations on temperature. However, as our experiments progressed, it seemed increasingly unlikely that our data could be interpreted in terms of carrier-density oscillations or, indeed, in terms of an *intraband* contribution to the dielectric constant. To understand the difficulties encountered in the interpretation of our experimental data in terms of the simple model of DM, this model, which has not been published previously, is presented in Sec. II. After discussing certain experimental details in Sec. III, the results of the laser magnetoreflection experiments are presented in Sec. IV. Possible interpretations of these results are discussed in Sec. V.

II. SIMPLE THEORY

In this section we will consider a simple theory of the optical SdH effect in which the reflectivity oscillations are caused by magnetic-field-dependent carrier-density oscillations. Starting with a very general expression for the optical conductivity, the intraband conductivity will be calculated for a sim-

ple model. This result will be used to evaluate the reflectivity as a function of the magnetic field and photon energy.

If the energy eigenvalues and eigenstates of an electron in a crystal are represented by E_i and $|i\rangle$, respectively, then the high-frequency conductivity $\sigma_{\gamma\beta}(\omega)$ can be expressed as a sum over states,

$$\sigma_{\gamma\beta}(\omega) = -e^2 \sum_{i,j} \frac{f(E_i) - f(E_j)}{E_i - E_j} \times \frac{\langle j|v_\gamma|i\rangle\langle i|v_\beta|j\rangle}{-i\omega + 1/\tau + (i/\hbar)(E_i - E_j)} , \quad (1)$$

where the summation indices i and j represent all the quantum numbers necessary to describe the initial and final states.[11] In Eq. (1), $f(E)$ is the Fermi function, $\vec{v}$ is the velocity operator, and τ is a relaxation time which is taken to be independent of the temperature, energy, and all external fields. In carrying out the sum over states, the expression $[f(E_i) - f(E_j)]/(E_i - E_j)$ is to be replaced by $(df/dE)|_{E=E_i}$ when $i=j$. Since the velocity operator may be written to include the effects of an external magnetic field and the effects of electron spin,[12] the above expression for the high-frequency conductivity should provide a suitable basis for the interpretation of high-field magnetoreflection experiments.[13,14]

To evaluate most simply the portion of Eq. (1) which is associated with the intraband conductivity, the carriers are assumed to be located in simple parabolic energy bands and the effects of electron spin are neglected. Although these assumptions are not valid for the carriers in antimony,[15] the results which are obtained here will allow us to examine the essential features of the dependence of the intraband conductivity on the magnetic field and photon energy.

To evaluate the intraband portion of Eq. (1) in the presence of a magnetic field, it is necessary to solve the Schrödinger equation in the effective-mass approximation:

$$(1/2m)\,\vec{\pi}\cdot\overleftrightarrow{\alpha}\cdot\vec{\pi}\,\Psi_n = E_n\Psi_n . \quad (2)$$

In Eq. (2), $\overleftrightarrow{\alpha}$ is the dimensionless inverse-effective-mass tensor, E_n are the energy eigenvalues measured from the bottom of the band in question, and $\vec{\pi}$ is related to the velocity operator $\vec{v}$ by

$$\vec{v} = \frac{\overleftrightarrow{\alpha}\cdot\vec{\pi}}{m} = \frac{\overleftrightarrow{\alpha}}{m}\cdot\left(\vec{p} + \frac{e}{c}\vec{A}_0\right), \quad (3)$$

where $\vec{p}$ is the electron momentum, m is the free-electron mass, and $\vec{A}_0$ is the vector potential of the external magnetic field.

Since the Fermi surface for the carriers in antimony is, for the purpose of this discussion, ellipsoidal and since the ellipsoids are tilted with respect to the crystallographic axes, the solution of Eq. (2) is greatly simplified by making a transformation in momentum space to a coordinate system in which the Fermi surface is spherical. We therefore introduce three real vectors $\vec{W}(1)$, $\vec{W}(2)$, and $\vec{W}(3)$ which are defined by the relation,[12,13]

$$\sum_{i=1}^{3} W_\gamma(i)\,W_\beta(i) = \alpha_{\gamma\beta} . \quad (4)$$

For electrons in a magnetic field, we impose the additional restrictions

$$\vec{W}(1)\times\vec{W}(3)\cdot\vec{H} = 0 , \quad (5a)$$

$$\vec{W}(2)\times\vec{W}(3)\cdot\vec{H} = 0 , \quad (5b)$$

$$\vec{W}(1)\times\vec{W}(2)\cdot\vec{H} < 0 , \quad (5c)$$

where $\vec{W}(3)$ is taken to be parallel to the magnetic field. For holes, the opposite inequality holds in Eq. (5c).

Using the $\vec{W}(i)$, it may be readily shown that the intraband conductivity for an arbitrary field direction is given by[13]

$$\sigma_{\gamma\beta}(\omega) = [W_\gamma(1)\,W_\beta(1) + W_\gamma(2)\,W_\beta(2)]\,\frac{n e^2\tau(1 - i\omega\tau)}{m[(1 - i\omega\tau)^2 + (\omega_c\tau)^2]} + [W_\gamma(2)\,W_\beta(1) - W_\gamma(1)\,W_\beta(2)]\,\frac{n e^2\tau\,\omega_c\tau}{m[(1 - i\omega\tau)^2 + (\omega_c\tau)^2]} + W_\gamma(3)\,W_\beta(3)\,\frac{n e^2\tau}{m(1 - i\omega\tau)} , \quad (6)$$

where the cyclotron frequency ω_c is defined by

$$\omega_c = \frac{eH}{m_c^* c} = \frac{eH}{mc}\left(\frac{\hat{b}\cdot\overleftrightarrow{m}\cdot\hat{b}}{\det\overleftrightarrow{m}}\right)^{1/2} , \quad (7)$$

in which $\overleftrightarrow{m} = (\overleftrightarrow{\alpha})^{-1}$ is the dimensionless effective-mass tensor, $\hat{b}$ is a unit vector along the magnetic field, and $\det\overleftrightarrow{m}$ is the determinant of the effective-mass tensor. In Eq. (6), the carrier density n is a function of the magnetic field H and the temperature T and is given by the expression[16]

$$n(H,T) = \frac{(2m_c^* E_F)^{3/2}}{3\pi^2\hbar^3}\left(\frac{m_H^*}{m_c^*}\right)^{1/2}\left(1 - \frac{3\pi\sqrt{2}}{4}\,\frac{kT(\hbar\omega_c)^{1/2}}{E_F^{3/2}} \times \sum_{p=1}^{\infty}\frac{(-1)^{p+1}\cos[(2\pi p E_F/\hbar\omega_c) + \frac{1}{4}\pi]\,e^{-2\pi^2 p kT_D/\hbar\omega_c}}{p^{1/2}\sinh(2\pi^2 p kT/\hbar\omega_c)}\right), \quad (8)$$

where T_D is the Dingle temperature and where the effective-mass projection along the magnetic field m_H^* is given by

$$m_H^* = (\hat{b}\cdot\overleftrightarrow{m}\cdot\hat{b})\,m . \quad (9)$$

In the absence of a magnetic field, Eq. (6) reduces to the usual zero-field result[17]

$$\sigma_{\gamma\beta}(\omega) = \frac{\alpha_{\gamma\beta} n_0 e^2\tau}{m(1 - i\omega\tau)} , \quad (10)$$

where n_0 is the zero-field carrier density, obtained by setting $H=0$ in Eq. (8).

When we calculate the reflectivity as a function of the magnetic field and photon energy, we will, for simplicity, consider the case where the magnetic field is parallel to the trigonal axis of the crystal and we will consider intraband effects due to both electrons and holes. Since the crystal has threefold symmetry about the trigonal axis, all of the electron and hole pockets will have the same cyclotron masses, though the electron masses will be about three times heavier than the hole masses[18]; thus, the oscillatory effects will be due primarily to holes. With the radiation normally incident on the crystal and parallel to the magnetic field, the intraband contribution to the dielectric constant becomes simply

$$\epsilon_{\mathrm{intra}}=\frac{4\pi i}{\omega}\,\sigma_{\mathrm{eff}}(\pm)$$

$$=\frac{4\pi i}{\omega}\left[\tfrac{1}{2}(\sigma_{11}+\sigma_{22})\pm\left\{\left[\tfrac{1}{2}(\sigma_{11}-\sigma_{22})\right]^2+\sigma_{12}\sigma_{21}\right\}^{1/2}\right]$$

$$=\frac{4\pi i}{\omega}\,\frac{e^2}{m}\left(\frac{3n_h(\alpha^h_{11}+\alpha^h_{22})\tau_h(1-i\omega\tau_h)}{(1-i\omega\tau_h)^2+(\omega_c^h\tau_h)^2}\right.$$

$$\left.+\frac{\frac{3}{2}n_e(\alpha^e_{11}+\alpha^e_{22})\tau_e(1-i\omega\tau_e)}{(1-i\omega\tau_e)^2+(\omega_c^e\tau_e)^2}\right)\ , \qquad (11)$$

where the subscripts 1 and 2 refer to the binary and bisectrix axes, respectively, and where the superscripts (or subscripts) e and h refer to electrons and holes, respectively. The normal-incidence reflectivity R can then be calculated using

$$R=\frac{(N-1)^2+K^2}{(N+1)^2+K^2}\ , \qquad (12)$$

where N and K are the real and imaginary parts of the index of refraction.

At this point we wish to consider the relationship between the temperature dependence of the reflectivity oscillations and the effective masses of the carriers. If the changes in the reflectivity with magnetic field are small (as our calculations for this simple model of the optical SdH effect suggest), we can make a Taylor expansion of the reflectivity in the quantity Γ, defined as

$$\Gamma=\Gamma(H,T)=\frac{n\tau(1-i\omega\tau)}{(1-i\omega\tau)^2+(\omega_c\tau)^2}\ , \qquad (13)$$

about its zero-field value

$$\Gamma_0=\Gamma(0,T)=\frac{n_0\tau}{1-i\omega\tau}\ . \qquad (14)$$

The reflectivity at a given magnetic field and temperature $R(H,T)$ is then given by

$$R(H,T)=R(0,T)+\left(\frac{\partial R}{\partial\Gamma}\right)_{\Gamma_0}(\Gamma-\Gamma_0)+\cdots\ . \qquad (15)$$

At the plasma edge, $\omega\tau\sim100$ and $(\omega_c/\omega)^2\sim\frac{1}{150}$ for $H=100$ kG, so that Γ is almost purely imaginary,

$$\mathrm{Im}\Gamma-\mathrm{Im}\Gamma_0=\omega\tau(\mathrm{Re}\Gamma-\mathrm{Re}\Gamma_0)$$

$$\cong\frac{\tau(\omega\tau)}{1+(\omega\tau)^2}\left((n-n_0)+\frac{n(\omega_c\tau)^2}{1+(\omega\tau)^2}\right)\ . \qquad (16)$$

Then we can write

$$\Delta R=R(H,T)-R(0,T)=\left(\frac{\partial R}{\partial\,\mathrm{Im}\Gamma}\right)_{\Gamma_0}(\mathrm{Im}\Gamma-\mathrm{Im}\Gamma_0)$$

$$\cong-\left(\frac{\partial R}{\partial\omega}\right)_{H=0}\frac{n_0}{\omega^3}\quad[(n-n_0)+n_0(\omega_c/\omega)^2]\ . \qquad (17)$$

Experimentally, we measure $[R(H,T)-R(0,T)]/R(0,T)$ so that the fractional change in the reflectivity is proportional to the oscillatory terms of Eq. (8) and to a nonoscillatory field-dependent term of comparable magnitude. Therefore, a study of the temperature dependence of the oscillatory-reflectivity amplitudes should yield the effective masses of the carriers associated with the oscillations.[1] Note that in Eq. (17) the coefficient of the term in large round brackets is multiplied by $(\partial R/\partial\omega)_{H=0}$, implying that structure in the zero-field reflectivity enhances the magnetic field dependence of the reflectivity. Hence the largest effects might be expected near the plasma edge.

Using parameters appropriate to antimony for the trigonal orientation, we have plotted in Fig. 1 the calculated fractional change in the reflectivity as a function of the magnetic field, assuming $T=0^\circ$K, for three photon energies near the plasma edge ($\hbar\omega_p\sim0.117$ eV). In each case, we see a series of oscillations, periodic in the inverse magnetic field, superimposed upon a field-dependent background which is rising or falling, depending upon the photon energy. For the upper two plots ($\hbar\omega=0.1033$, 0.1127 eV), the passage of a Landau level through the Fermi surface is associated with the reflectivity minima, while for the lowest plot ($\hbar\omega=0.1181$ eV) it is associated with the reflectivity maxima. Note that the magnetic field values associated with the passage of a Landau level through the Fermi surface (hereafter referred to as dHvA resonant-field values) are independent of the photon energy. This frequency-independent feature of their experimental data led DM to associate the periodic reflectivity oscillations with the optical SdH effect.[10]

The cusps in the carrier density [and, from Eq. (17), in the reflectivity] occur, for our model, when a Landau level l passes through the Fermi surface:

$$E_F=\hbar\omega_c(l+\tfrac{1}{2})\ . \qquad (18)$$

More generally, Onsager[19] has shown that the passage of a Landau level through the Fermi surface occurs when

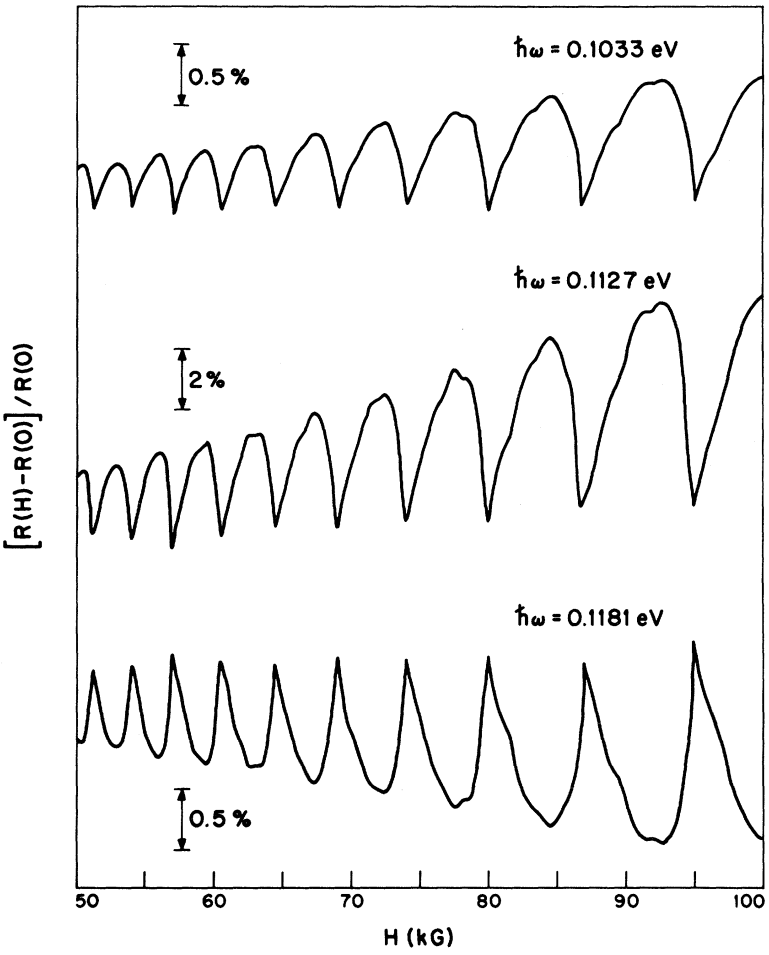

FIG. 1. Calculated reflectivity spectrum for antimony at the photon energies 0.1033, 0.1127, and 0.1181 eV, assuming $T = 0$ °K, for the magnetic field parallel to the trigonal axis. For the top two traces, the passage of a Landau level through the Fermi surface is associated with the reflectivity *minima*, while for the bottom trace, the reflectivity *maxima* correspond to the passage of a Landau level through the Fermi surface.

$$\frac{1}{PH} = \frac{cA_F}{2\pi e\hbar H} = l + \gamma \,, \tag{19}$$

where P is the dHvA period, A_F is the area of a stationary section of the Fermi surface taken normal to the magnetic field, and γ is the phase of the carriers.

The fine structure on the main oscillations of Fig. 1 is associated with the electrons. The effects due to electrons are small, since for this magnetic field orientation, the cyclotron mass for the electrons is much larger than that for the holes.

In Fig. 2, the amplitudes of the reflectivity oscillations which occur near 87 kG (see Fig. 1) are plotted as a function of photon energy. The positive and negative reflectivity amplitudes indicate that the passage of a Landau level through the Fermi surface is associated with reflectivity minima and maxima, respectively. We notice that the amplitudes of the reflectivity oscillations are only sizeable in the vicinity of the plasma edge. For our simple model, this can be understood from Eq. (17). More generally, the real part of the dielectric constant vanishes near the plasma edge when the core dielectric constant cancels the real part of the zero-field intraband dielectric constant (or the imaginary part of the intraband conductivity). When this occurs, the small conductivity oscillations (about 1% for magnetic fields near 100 kG) give rise to observable reflectivity oscillations.

For comparison with our simple theory, we present, in Fig. 3, an experimental trace obtained by DM, using a globar source. The magnetic field is along the binary axis, the sample temperature is about 25 °K and the photon energy is 0.1086 eV, which is very close to the plasma edge. We see the small SdH oscillations superimposed on a large field-dependent background. Since this trace is so noisy, the asymmetry in the line shape associated with the passage of a Landau level through the Fermi surface cannot be observed. However, using the fact that the field-dependent background is rising, the dHvA resonant fields are identified with reflectivity minima (see Fig. 1). The period obtained by fitting the dHvA resonant fields to an expression like Eq. (19) agrees well with the electron period

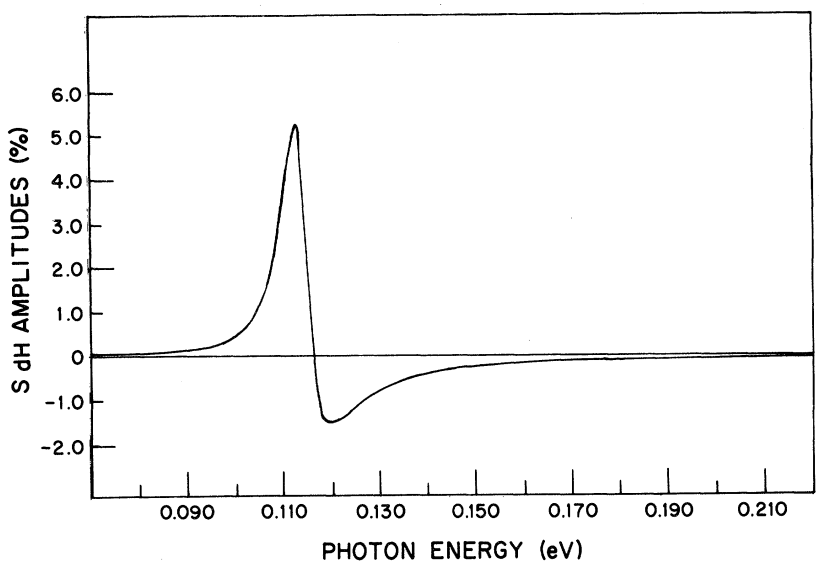

FIG. 2. Calculated fractional change in the reflectivity associated with the passage of the $l = 11$ Landau level through the Fermi surface as a function of photon energy, for antimony with the magnetic field parallel to the trigonal axis. Positive and negative values indicate that the passage of a Landau level through the Fermi surface is associated with reflectivity minima and maxima, respectively.

measured by Windmiller for this orientation.[3]

As we mentioned previously, DM found that the magnetic field values associated with the reflectivity extrema were independent of the photon energy. They also found indirect evidence that the dHvA resonant fields were associated with reflectivity minima below the plasma frequency and reflectivity maxima above the plasma frequency. Furthermore, the range of photon energies over which they observed the SdH reflectivity oscillations corresponds to the range predicted by the simple theory outlined above. However, in spite of the agreement between theory and experiment on the line-shape reversal at the plasma frequency, the general shape of the frequency dependence of the oscillatory amplitudes and the range of frequencies for which the SdH oscillations are observed, there is some disagreement about the magnitudes of the oscillatory amplitudes. The magnitudes of the oscillatory reflectivity amplitudes, as computed using Eqs. (8) and (17) for $T = 25\,^{\circ}\mathrm{K}$, are about two orders of magnitude smaller than those observed by DM.

The present experiments were undertaken to check this agreement in a more quantitative sense. If the asymmetry in the line shape could be observed, then a more precise determination of the dHvA periods would be possible. Furthermore, from a study of the temperature dependence of the oscillatory amplitudes, the effective masses of the carriers associated with the oscillations could be determined, as one usually does in dHvA experiments[1]; such a study could provide excellent proof that the reflectivity oscillations observed by DM are associated with dHvA-like oscillations in the optical conductivity. Finally, the apparent problem with the magnitude of the reflectivity oscillations indicated the need for further investigation.

III. EXPERIMENTAL APPARATUS AND SAMPLE PREPARATION

The experimental apparatus employed in the pres-

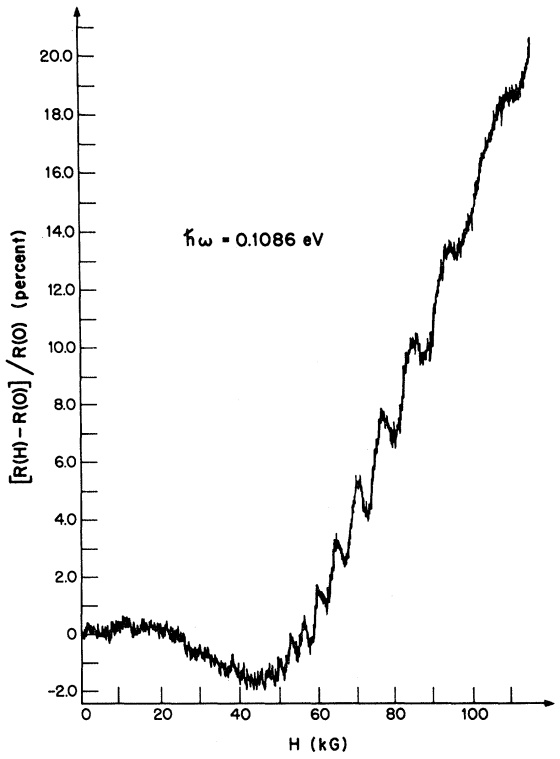

FIG. 3. Experimental trace of Dresselhaus and Mavroides (Ref. 10) showing the fractional change in the reflectivity plotted as a function of the magnetic field for the magnetic field along the binary axis. Photon energy is 0.1086 eV and the sample temperature is about 25 °K.

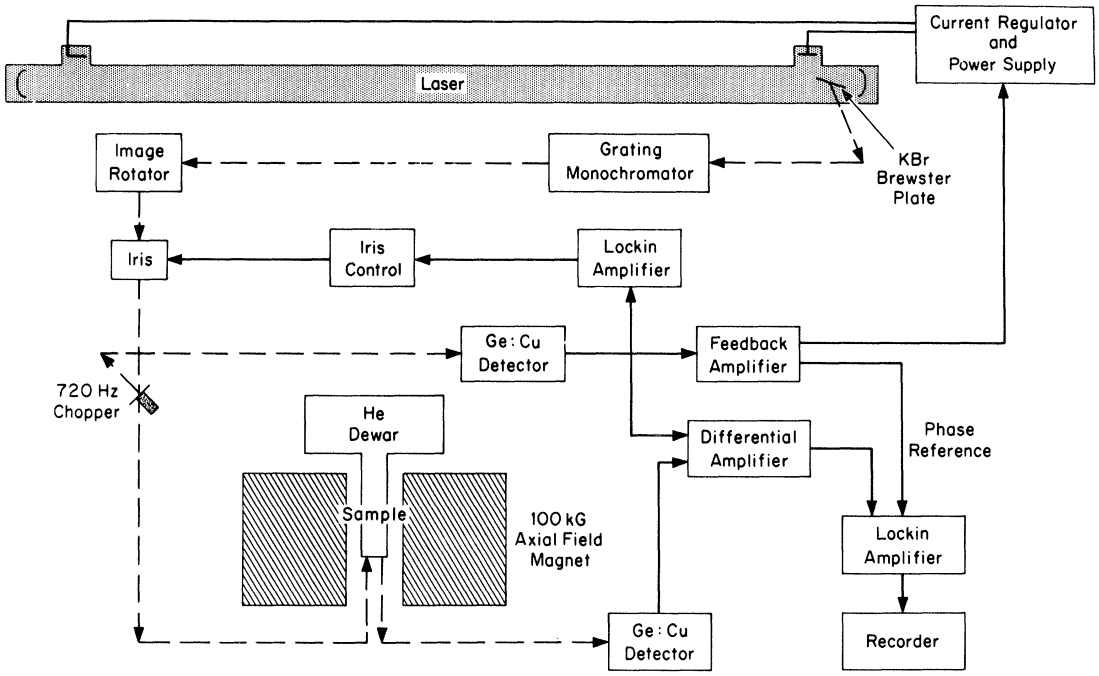

FIG. 4. Experimental apparatus used in the laser magnetoreflection experiments.

ent experiments contains two substantial improvements over that used by DM.[10] These are (i) the use of an amplitude-stabilized laser instead of a globar source and (ii) the use of a sample Dewar which allows the immersion of the sample in liquid helium. The focusable laser beam permits the use of smaller samples and thereby leads to a reduction in magnetic field inhomogeneities over the sample and a subsequent increase in the magnitudes of the oscillatory-reflectivity amplitudes. The higher resolution, furthermore, makes possible experimental line-shape studies. The second experimental modification, which made possible measurements on samples at low temperatures (~2 °K), turned out to be most significant and is discussed in Sec. IV.

A block diagram of the experimental setup is shown in Fig. 4. The laser uses Ne, He-Ne, and He-Xe gas mixtures to produce a number of lines with wavelengths between 3.5 and 18.5 μ. The beam is coupled out of the laser by means of a Brewster-angle plate and is, therefore, linearly polarized. One laser line is selected by means of a low-resolution monochromator and this line passes through an image rotator which allows one to vary the polarization of the optical electric field with respect to the crystallographic axes of the sample. The beam then passes through an iris diaphragm whose aperture is controlled by an error signal from the Ge:Cu reference detector. This serves to control the long-time-constant laser drift. The beam is chopped at 720 Hz, with half of the beam being reflected from the chopper blade and passing to a reference detector. The other half of the beam passes through the chopper blade, is reflected from the sample which is immersed in liquid He, and is detected by another Ge:Cu detector. The signals from the two detectors are subtracted in a difference amplifier and the result is sent to a lock-in amplifier whose output is recorded on a chart recorder. The laser output is regulated by controlling the laser current with an error signal generated by the feedback amplifier.[14] Using both the iris diaphragm and the feedback-current regulator, the laser output can be stabilized to better than 1% over a period of $\frac{1}{2}$ h.

The most formidable experimental problems encountered in the course of this work were those related to sample preparation. It was found that the experimental results depended critically on the surface quality as well as upon the previous history of the sample. When a "good" sample surface was prepared, the magnetoreflection traces obtained at sample temperatures near 2 °K resembled those shown in Fig. 9 of Sec. IV where the large SdH oscillations are the dominant features in the reflectivity. When a "bad" surface was prepared, the traces obtained at low temperatures resembled the trace of DM shown in Fig. 3, where the small SdH oscillations are observed in the reflectivity only for frequencies in the vicinity of the plasma edge. The standard method of checking a sample surface by examining the spots in a Laue x-ray backreflection picture proved to be insensitive to the differ-

ences between the sample surfaces which yielded good results and those which did not.

The most important consideration in obtaining good results is the use of material which has not been temperature cycled, since the quality of a sample deteriorates rapidly with thermal cycling. After yielding good optical SdH results at liquid-helium temperatures, a sample which is warmed to room temperature and then recooled to liquid-helium temperatures yields nothing. Subsequent attempts to resurface material which has been cycled have proven fruitless, indicating that the entire crystal is strained. When a good sample was found, it was kept at liquid-nitrogen temperatures until the next magnet run, after which it was again preserved at liquid-nitrogen temperatures. Even with these precautions, samples deteriorated rapidly and the SdH amplitudes decreased significantly from one day to the next.[20] Of course, extreme caution was exercised in mounting the samples. A small beryllium-copper spring was used to hold the samples in place, after which a small quantity of vacuum grease was applied to keep the samples from moving about.

All experiments were performed on samples with surfaces perpendicular to one of the principal crystallographic axes. Trigonal faces were prepared by cleaving the material in liquid nitrogen and immediately etching the surface for about 30 sec in a bath consisting of six parts glacial-acetic acid, five parts fuming-nitric acid, and two parts hydrofluoric acid. The preparation of sample surfaces perpendicular to the binary and bisectrix axes presented more of a problem. The most effective method involved hand-lapping the surfaces, using SiC grits of various sizes with water on a glass plate. After being lapped with the finest grit, the samples were treated with the above-mentioned etch. The sample was then lapped again for a shorter time, using the finer grits, and etched again. This process was repeated four or five times, each time reducing the lapping time and the size of the grit. Samples prepared in this manner possessed a fine optical surface and had a reasonably good chance of yielding interesting optical SdH results.[20]

IV. EXPERIMENTAL RESULTS

In this section the results of the laser magneto-reflection studies of the optical SdH effect will be presented and discussed. We will find that, at low temperatures, with good samples, our results differ in two major respects from the predictions of the simple model of Sec. II. First of all, for magnetic fields near 100 kG, fractional changes in the reflectivity as large as 100% are observed when a Landau level passes through the Fermi surface. We remarked at the end of Sec. II that the SdH oscillatory amplitudes observed by DM were much larger than one would expect to find at the temperature of their experiments. At low temperatures, the magnitudes of these oscillations become very strikingly large. The second major discrepancy between our simple model and our experimental observations is in the weak dependence of the oscillatory-reflectivity amplitudes on photon energy. We observe large fractional changes in the reflectivity over the entire range of photon energies available from our laser ($0.0670 < \hbar\omega < 0.3655$ eV). In particular, we find the amplitudes to be roughly independent of energy throughout the entire energy range, although, on the best samples, the SdH amplitudes increase slightly with increasing energy. In addition, we observe a number of other new phenomena, usually on those samples which exhibit the largest SdH oscillations.

A. Binary Orientation

We first wish to consider the orientation for which the binary axis is parallel to the magnetic field. For this orientation, the various hole and electron ellipsoids will not be equivalent and the intraband contribution to the dielectric constant will no longer have the simple form of Eq. (11). For the binary orientation, the largest dHvA periods are associated with the nonprincipal hole and electron ellipsoids[21] and have the values 1.16×10^{-6} and 1.27×10^{-6} G^{-1}, respectively.[3] The effective conductivity for this orientation is[17]

$$\sigma_{\rm eff}(\pm) = \tfrac{1}{2}(\sigma_{22}+\sigma_{33}) \pm \{[\tfrac{1}{2}(\sigma_{22}-\sigma_{33})]^2 + \sigma_{23}\sigma_{32}\}^{1/2}, \tag{20}$$

where the subscripts 2 and 3 refer to the bisectrix and trigonal axes, respectively, and where, in the absence of a magnetic field, the + sign is chosen to give the conductivity for the optical electric field parallel to the bisectrix axis and the − sign to give the conductivity for the electric field parallel to the trigonal axis.

Evaluating the $\vec{W}$ vectors for the nonprincipal ellipsoids, the intraband-conductivity components appearing in Eq. (20) may be found using Eq. (6). They are for electronic conduction

$$\sigma_{22}/\sigma_0 = \tfrac{1}{4}(3\alpha_{11}+\alpha_{22}), \tag{21a}$$

$$\sigma_{33}/\sigma_0 = \alpha_{33}, \tag{21b}$$

$$-\sigma_{23}/\sigma_0 = +\sigma_{32}/\sigma_0 = \tfrac{1}{2}[\alpha_{33}(3\alpha_{11}+\alpha_{22}) - \alpha_{23}^2]^{1/2} \times[\omega_c\tau/(1-i\omega\tau)], \tag{21c}$$

where

$$\sigma_0 = \frac{qne^2\tau(1-i\omega\tau)}{m[(1-i\omega\tau)^2+(\omega_c\tau)^2]}, \tag{22}$$

and where q is the number of nonprincipal carrier ellipsoids for each kind of carrier and has the value 2 for electrons and 4 for holes. [Note that for holes,

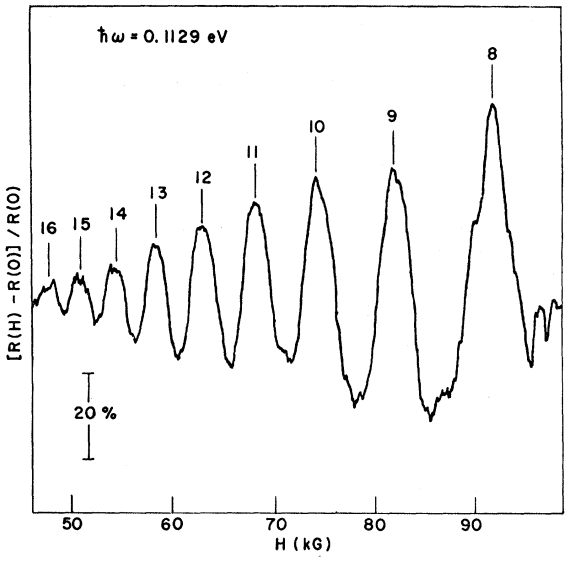

FIG. 5. Experimental magnetoreflection trace obtained at $\hbar\omega = 0.1129$ eV and $T = 1.89$ °K, with $\vec{H}$ parallel to the binary axis and polarization $\vec{E}$ parallel to the bisectrix axis.

the opposite signs are taken in Eq. (21c).] Using appropriate values for the inverse-effective-mass-tensor components[18] and assuming the electron and hole relaxation times to be comparable, the contribution to the effective conductivity from the nonprincipal hole and electron ellipsoids can be evaluated. It is found that the contribution from the hole ellipsoids is comparable to, though slightly larger than, the contribution from the electron ellipsoids. Thus, if the hole and electron relaxation times are comparable, we should observe two series of SdH oscillations in the reflectivity, with the amplitudes of the oscillations associated with the holes being slightly larger than those associated with the electrons.

The experimental trace for H parallel to the binary axis shown in Fig. 5 was obtained for a wavelength of 10.978 μ (= 0.1129 eV) which is very close to the plasma edge; the sample temperature was 1.89 °K and electric field polarization was E parallel to the bisectrix axis. In sharp contrast to the trace of Fig. 3, the trace of Fig. 5 shows a single series of extremely large reflectivity oscillations which completely wash out the magnetic-field-dependent background. Near 90 kG, the amplitude of these reflectivity oscillations reaches nearly 70%, which is more than an order of magnitude larger than the predictions of the simple theory of Sec. II.

Using the fact that the passage of a Landau level through the Fermi surface is associated with the narrow sharp portion of oscillatory line shape (see the discussion following Fig. 2), we can identify the dHvA resonant magnetic fields with the reflectivity maxima and make a quantum assignment as shown in Fig. 5. Using this quantum assignment and the dHvA resonant-field values, a least-squares fit was made to Eq. (19) to determine the period P and the phase γ associated with the oscillations labeled 8–16 in Fig. 5. We obtain $P = 1.24 \times 10^{-6}$ G^{-1}, which agrees well with the period measured by Windmiller[3] for electrons.

Using standard expressions,[22] we computed the standard deviation in magnetic field, Δ_H, and the fractional standard deviation in the period, $\Delta P/P$, due to differences between the data points and the fitted line. For the trace of Fig. 5 we obtain $\Delta_H = 305$ G and $\Delta P/P = 0.83\%$. Since the experimental traces can be read to 0.1% of full scale, or about 100 G, we see that the deviation of the data points from the fitted line is rather large compared with the accuracy to which we can read the experimental traces. However, this is to be expected since the reflectivity maxima of Fig. 5 are rather broad. Note that the absolute accuracy of our magnetic field values is not greater than 1%. Furthermore, the magnet calibration tends to change slightly with time because of shifts in the copper plates which make up the Bitter solenoid. Nevertheless, it is interesting and useful to calculate Δ_H in order to check the internal consistency of our least-squares fit with regard to the quantum assignment and to the identification of the dHvA resonant fields with either reflectivity minima or maxima. Thus, the value we have calculated for $\Delta P/P$ is not to be taken as the absolute error in the period measurement. Instead, this value is useful for checking the periodicity of the reflectivity oscillations in inverse magnetic field. The fits to the experimental traces which are presented below yield even smaller values for $\Delta P/P$ than the fit to the trace of Fig. 5, indicating that the periodicity of the reflectivity oscillations in inverse magnetic field is quite exact, even for these low quantum numbers. Since we expect the departures from periodicity to be minor as long as the Fermi level does not depend strongly upon the magnetic field, the small values we obtain for $\Delta P/P$ indicate that it is a good assumption to take the Fermi level to be independent of the magnetic field for $H < 100$ kG.

The exact periodicity of the reflectivity oscillations in inverse magnetic field also supports the observation that the reflectivity oscillations are associated with a single set of conductivity oscillations, due to electrons. When we examine traces for the bisectrix orientation below, we will see that the presence of two series of conductivity oscillations will give rise to reflectivity oscillations which exhibit sizeable departures from periodicity as evidenced by large values for $\Delta P/P$. From our previous discussion, it is difficult to understand the absence of reflectivity oscillations associated with

holes on the trace of Fig. 5. The zero-field reflectivity calculations,[23] which gave the electron and hole relaxation times used to obtain the plots of Figs. 1 and 2, indicate that the relaxation times for electrons and holes are roughly equal. Although we would expect to observe reflectivity oscillations due to both electrons and holes, we find no evidence for oscillations due to holes on the trace of Fig. 5 or on any other experimental trace obtained from the same sample at other photon energies. A solution to this dilemma will be proposed when we examine data for the bisectrix orientation below.

As we remarked previously, the amplitudes of the SdH reflectivity oscillations in the trace of Fig. 5 are more than an order of magnitude larger than the reflectivity oscillations which are to be expected from carrier-density oscillations in the intraband conductivity. For the carriers in antimony, the carrier-density oscillations have amplitudes of about 1% at $T = 0\,^{\circ}\mathrm{K}$ for magnetic fields near 100 kG and it is the plasma-edge enhancement of the oscillatory component of ϵ_1 which leads to SdH oscillations in the reflectivity of 5% near the plasma edge. The large amplitudes of the observed reflectivity oscillations lead us to believe that the oscillations are probably associated with some mechanism other than carrier-density oscillations. In this regard, the dc SdH experiments of Rao *et al.*[5] and Long *et al.*[6] are very suggestive. Rao *et al.*[5] observed SdH oscillations in antimony due to both electrons and holes and they noticed that the amplitudes of these oscillations were nearly two orders of magnitude larger than one would expect on the basis of a theory which only considered magnetic-field-dependent variations in the carrier density and the Fermi level, such as that of Lifshitz and Kosevitch.[24] Their experimental results were also compared with the predictions of a theory due to Zil'berman,[25] who considered the effects of Landau quantization on the relaxation times of the carriers. The predictions of the Zil'berman theory were somewhat larger than the observed amplitudes, but were of the correct order of magnitude. Long *et al.*[6] reached similar conclusions in regard to their SdH experiments. We note that an energy-dependent relaxation time would lead to a different functional form for the intraband conductivity. However, we will defer further consideration of this problem until more experimental data have been presented.

Finally, it is interesting to note that in Fig. 5 there are no signs of the large field-dependent background which appears in the trace of Fig. 3. Although the amplitude of this background in Fig. 3 reaches 20% at magnetic fields near 100 kG, it is not visible in the trace of Fig. 5. It is also important to note that the resonant line shapes in Fig. 5 indicate that the passage of Landau levels through the Fermi surface is associated with reflectivity maxima, even though the photon energy at which the trace of Fig. 5 was obtained is below the plasma energy (~ 0.117 eV). Furthermore, the dHvA resonant magnetic fields are associated with reflectivity maxima on all experimental traces (that is, at all photon energies) obtained from this particular sample, as the line shape and the values obtained for Δ_H and $\Delta P/P$ indicate.

It is not always the case that the resonances are identified with reflectivity maxima, as can be seen in the traces of Fig. 6. The top trace of Fig. 6 was obtained at a wavelength of 18.500 μ (= 0.0670 eV), while the bottom trace was obtained for a wavelength of 5.5739 μ (= 0.2224 eV). In both cases, the sample temperature was around $1.96\,^{\circ}\mathrm{K}$ with the optical electric field E parallel to the bisectrix axis. Although the photon energies at which both of these traces were obtained are far from the plasma energy, we nevertheless observe SdH reflectivity oscillations with extremely large amplitudes. In each trace, there is a single series of oscillations, although it is the reflectivity minima that are now associated with the passage of a Landau level through the Fermi surface.

Using the quantum assignment shown in Fig. 6, a fit was made to the reflectivity minima to obtain the period and phase. For the bottom trace, we obtain $P = 1.28 \times 10^{-6}\ \mathrm{G}^{-1}$ with $\Delta_H = 380$ G and $\Delta P/P = 0.97\%$, while, for the top trace, $P = 1.28 \times 10^{-6}\ \mathrm{G}^{-1}$ with $\Delta_H = 330$ G and $\Delta P/P = 0.83\%$. In both cases, a fit was made to the reflectivity minima labeled 8–17. Although the fit is rather good, we notice, in the bottom trace, that the reflectivity minima labeled 15–17 are less clearly defined than the others and contribute most significantly to Δ_H. We confirm this by making a fit to the minima of the lower trace corresponding to $l = 8$–14; we obtain $\Delta_H = 176$ G and $\Delta P/P = 0.55\%$. This value for Δ_H is close to the accuracy with which we can read the experimental traces, and the small value for $\Delta P/P$ indicates the exactness of the periodicity of the reflectivity oscillations in inverse magnetic field, leaving little doubt that the reflectivity oscillations in the bottom trace of Fig. 6 are associated with electrons only. Similar conclusions apply to the top trace of Fig. 6.

The traces of Fig. 6 disclose, in a clear and obvious manner, the second major discrepancy between our experimental data and the predictions of the simple theory of Sec. II. In the bottom trace, for example, the amplitudes of the reflectivity oscillations near 75 kG are around 40%, whereas the simple theory suggests that they should be on the order of 0.1%. Similarly, in the upper trace of Fig. 6, the amplitudes of the reflectivity oscillations are nearly two orders of magnitude larger than the predictions of the simple theory. Considering the traces of Fig. 6 along with other traces obtained

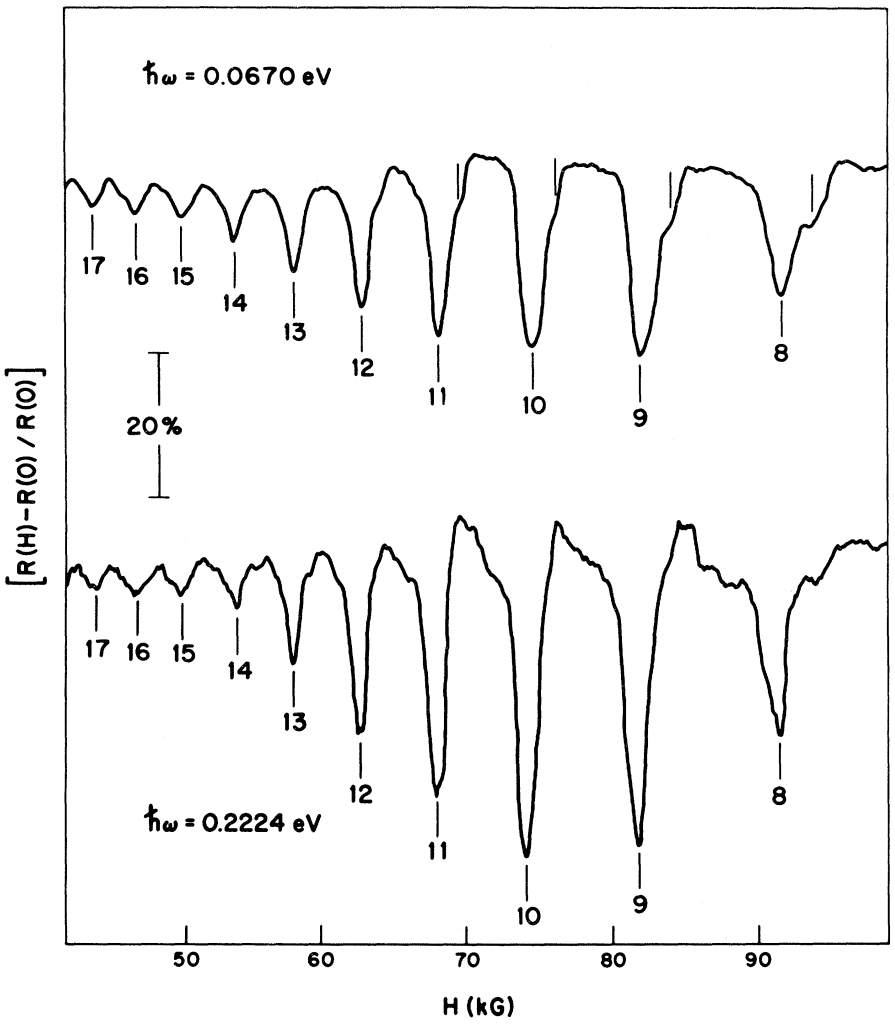

FIG. 6. Experimental magnetoreflection traces obtained at $\hbar\omega = 0.0670$ and 0.2224 eV for $T = 1.96\,^{\circ}\mathrm{K}$, $\vec{H}$ parallel to the binary axis and polarization $\vec{E}$ parallel to the bisectrix axis.

from the same sample, we find that the amplitudes of the reflectivity oscillations are roughly independent of the photon energy (to within a factor of 2) and they are observed over a very wide range of photon energies, not just in the vicinity of the plasma edge as previously reported[10] and predicted by the simple theory. Furthermore, the strong photon energy dependence of $\epsilon_1 \sim 1/\omega^2$ for intraband processes implies that this contribution to ϵ_1 must become extremely small at photon energies much greater than the plasma energy, so that smaller reflectivity oscillations are expected at high photon energies than at low energies. However, we find this not to be the case and, in Fig. 6, the reflectivity oscillations observed at 0.2224 eV are, in fact, larger than those obtained at 0.0670 eV.

The presence of large-amplitude reflectivity oscillations at photon energies well above (and below) the plasma energy is a feature which is common to all samples of reasonably high quality. For the sample of Fig. 6 we observe that there is no line-shape reversal associated with the plasma energy and the resonances are associated with reflectivity minima for photon energies both above and below the plasma energy. We remarked in connection with the sample which yielded the trace of Fig. 5 that the dHvA resonant fields were associated with reflectivity maxima for all photon energies (both above and below the plasma energy). In general, it has been found for high-quality samples that the passage of a Landau level through the Fermi surface is associated with either reflectivity minima or maxima, depending upon the sample, and that no line-shape reversal occurs at the plasma energy. None of these phenomena can be understood in terms of the simple theory of Sec. II.

We note briefly that the envelope on the SdH oscillations in the traces of Fig. 6 is probably due to a beating between contributions from the two electron ellipsoids. A 3° misalignment of the binary axis and the magnetic field would give rise to a 5% difference between the dHvA periods of the two

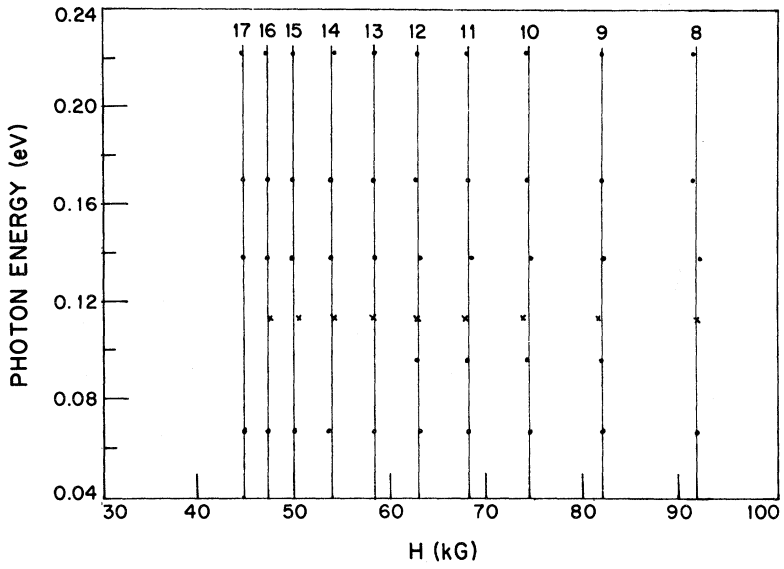

FIG. 7. Frequency independence of the dHvA resonant fields is seen in this plot of the dHvA resonant magnetic field values as a function of photon energy.

electron ellipsoids,[3] and this would be enough to explain the envelope. Such a misalignment is possible because of the surface preparation and sample alignment procedures.

On the upper trace of Fig. 6 ($\hbar\omega = 0.0670$ eV), we have marked some additional structure on the high-field side of the reflectivity minima labeled 8–11. This series of shoulders is periodic in inverse magnetic field with a period equal to that of the main reflectivity minima 8–14. If these shoulders are associated with the spin splitting of the Landau levels, and the cyclotron-mass data of Datars and Vanderkooy[18] are used to compute the g factors associated with this splitting, reasonable agreement is obtained with the g factors determined by Windmiller[3] and McCombe and Seidel.[8] Because of the crystal misalignment in the results of Fig. 6, it would be unwise to place great emphasis of these values for the g factors. This point will be considered again when data for the trigonal orientation are presented. Finally, for the traces of Fig. 6, it is important to note that the magnetic field value at which a given Landau level passes through the Fermi surface is independent of the photon energy. It was this frequency independence of the dHvA resonant fields which led DM to identify the reflectivity oscillations with the optical SdH effect. To emphasize this point, the dHvA resonant-field values from experimental traces, obtained from the sample which gave the traces of Fig. 6, are plotted in Fig. 7. The quantum assignment for the resonant-field values is given above the vertical lines. The frequency independence of the resonant-field values, over a very large photon-energy range, leaves little doubt that the reflectivity oscillations are associated with a dHvA-like mechanism in the optical conductivity. Of course, similar plots can be made for data obtained from other binary samples as well as from samples for other crystallographic orientations and the frequency independence of the resonant fields is observed for these data as well.

The oscillatory-reflectivity amplitudes were found to be independent of temperature below 2.1 °K, although they were observed to increase in magnitude as the temperature was lowered from 4.2 to 2.1 °K. However, because of the noise on the experimental traces from the He bubbles in the sample Dewar for temperatures above the λ point of He, no quantitative information was obtained. It is also interesting that for measurements at higher temperatures (~20 °K) or on samples of lower quality, a line-shape reversal in accordance with the simple theory is observed.[20]

B. Bisectrix Orientation

We will now consider the orientation where the magnetic field is parallel to the bisectrix axis. For this orientation, the principal-carrier ellipsoids for both electrons and holes will have the smallest cyclotron masses and, therefore, the largest dHvA periods. Windmiller[3] finds the dHvA periods associated with the principal hole and electron ellipsoids to be 1.32×10^{-6} and 1.47×10^{-6} G^{-1}, respectively. For the bisectrix orientation, none of the off-diagonal components of the conductivity tensor vanish by symmetry alone,[26] so that the characteristic modes for the propagation of an electromagnetic wave into the crystal are not entirely transverse.[27] Thus, the expression for the effective conductivity will no longer have the simple form of Eq. (20). Evaluating the $\tilde{W}$ vectors for the principal ellipsoids, we obtain, for the bisectrix orientation,

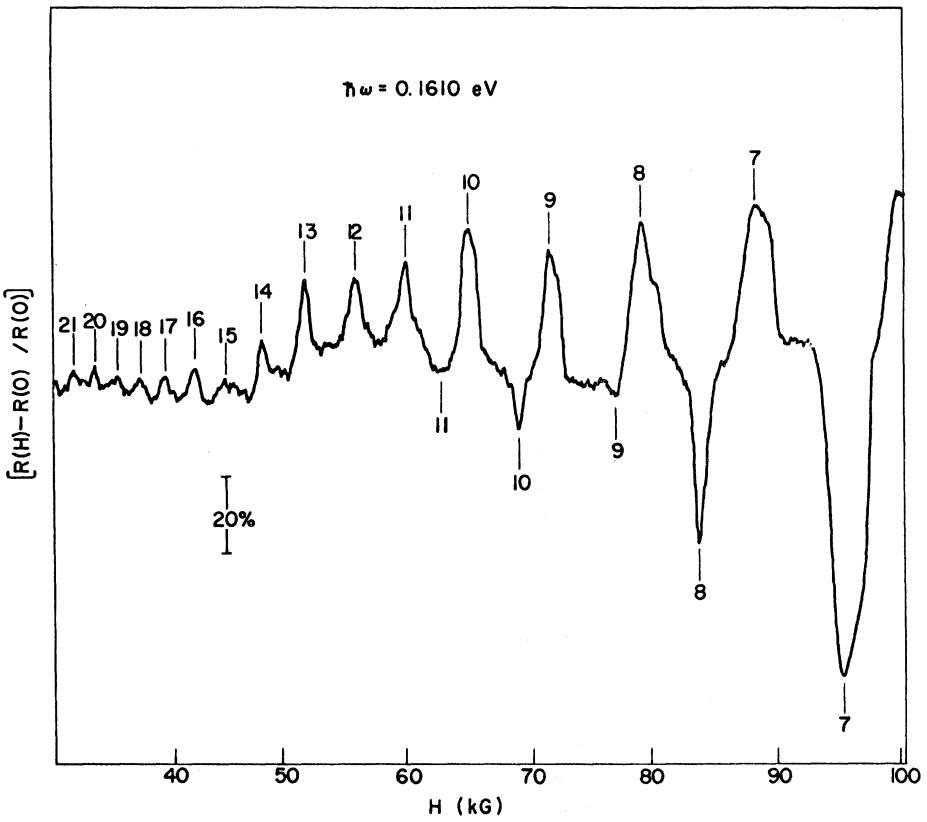

FIG. 8. Experimental magnetoreflection trace obtained at $\hbar\omega = 0.1610$ eV, $T = 1.95\,^{\circ}$K, $\vec{H}$ parallel to the bisectrix axis and the polarization $\vec{E}$ parallel to the binary axis. Reflectivity maxima are associated with electrons and the minima with holes.

$$\sigma_{11}/\sigma_0 = \alpha_{11}\,, \tag{23a}$$

$$\sigma_{33}/\sigma_0 = \alpha_{33}\,, \tag{23b}$$

$$-\sigma_{13}/\sigma_0 = +\sigma_{31}/\sigma_0 = (\alpha_{11}\,\alpha_{33})^{1/2}\,\omega_c\tau/(1 - i\omega\tau)\,, \tag{23c}$$

$$-\sigma_{12}/\sigma_0 = +\sigma_{21}/\sigma_0 = (\alpha_{11}/\alpha_{33})^{1/2}\,\alpha_{23}\,\omega_c\tau/(1 - i\omega\tau)\,,$$

$$\sigma_{23}/\sigma_0 = \sigma_{32}/\sigma_0 = 0\,, \tag{23d}$$

where σ_0 is given by Eq. (22) and where q is now the number of principal carrier ellipsoids for each kind of carrier, so that $q = 1$ for holes and $q = 2$ for electrons. The subscripts 1, 2, and 3 refer to the binary, bisectrix, and trigonal axes, respectively. The signs given in Eqs. (23c) and (23d) are correct for electrons and the opposite signs apply to holes. Evaluating the above combinations of inverse-effective-mass-tensor components, it is found that the coupling between the transverse and longitudinal directions, which is governed by σ_{12}, is not entirely negligible at the highest fields at which useful data were obtained ($H = 100$ kG). However, since $(\omega_c/\omega)^2 \sim \frac{1}{150}$ at the plasma edge for $H = 100$ kG, the conductivity can be approximated for this discussion by

$$\sigma_{\mathrm{eff}}(\pm) \cong \tfrac{1}{2}(\sigma_{11} + \sigma_{33}) \pm \{[\tfrac{1}{2}(\sigma_{11} - \sigma_{33})]^2 + \sigma_{13}\,\sigma_{31}\}^{1/2}\,, \tag{24}$$

where the + sign is taken for E parallel to the binary axis and the – sign is taken for E parallel to the trigonal axis.

Using Eq. (24), it can be shown that the major contributions to the effective conductivity from the electron and hole principal-carrier ellipsoids will be comparable if the electron and hole relaxation times are comparable. This is essentially the same result that was predicted by the simple model for the binary orientation. In fact, in the absence of a magnetic field, the reflectivity of a bisectrix face is identical to that of a binary face.[23] However, in the presence of a magnetic field, we should expect differences between the binary and bisectrix orientations, since, for example, the cyclotron masses associated with the ellipsoids giving rise to the largest dHvA periods are lighter for the bisectrix orientation than for the binary orientation.

We now wish to consider an experimental trace for the bisectrix orientation. In Fig. 8, we present a trace which was obtained for a laser wavelength of 7.6994 μ (= 0.1610 eV) and a sample temperature of 1.95 °K, with E parallel to the binary axis. We notice two series of reflectivity oscillations, one associated with reflectivity minima and the other with reflectivity maxima. Since the presence of two sets of conductivity oscillations will give rise to reflectivity oscillations which are not exactly periodic in inverse magnetic field, we first con-

sider the magnetic field region below 60 kG, where the data show only one set of reflectivity oscillations. Making a quantum assignment for these maxima, we determine the period, using the maxima labeled 12–18. We obtain $P = 1.47 \times 10^{-6}$ G^{-1}, which compares well with Windmiller's results for electrons. For these resonances, we also obtain $\Delta_H = 145$ G and $\Delta P/P = 0.69\%$, which compare favorably with the values obtained for the same quantities for the binary traces. If we now make a fit to the reflectivity minima labeled 7–11, we find $P = 1.34 \times 10^{-6}$ G^{-1} which is in good agreement with Windmiller's results for holes. However, for these reflectivity minima, there are sizeable departures from periodicity since $\Delta_H = 815$ G and $\Delta P/P = 2.35\%$. Our identification of the reflectivity maxima with electrons and the reflectivity minima with holes is corroborated by an experimental trace of McCombe and Seidel[8] of magnetothermal oscillations for the bisectrix orientation.

Having identified these two sets of reflectivity oscillations, it is interesting to consider some other features of the trace of Fig. 8. The most striking feature, in light of our previous discussion, is that the electron oscillations are associated with reflectivity maxima while the hole oscillations are associated with reflectivity minima. This was found to be true for E parallel to the binary axis, regardless of photon energy, for all experimental traces obtained from this sample. This phenomenon contradicts the predictions of our simple model, which says that the dHvA resonant fields associated with both electrons and holes should correspond to either minima or maxima in the reflectivity, depending only upon the photon energy.

Another interesting feature of this trace is to be seen in the magnetic field dependence of the oscillatory amplitudes for the two carriers. The oscillations associated with electrons are observed at magnetic fields as low as 30 kG. However, the oscillations associated with holes disappear entirely below 60 kG, although the amplitude of the $l = 7$ minimum near 95 kG is almost 90%. This means that the relaxation time for holes must possess a very strong dependence upon the magnetic field, whereas the gradual decrease of the electron amplitudes with decreasing field indicates a much weaker field dependence for the electron relaxation time. This strong dependence upon the magnetic field is observed at all photon energies for the reflectivity oscillations associated with holes.

Keeping in mind the similarities between the binary data and the bisectrix data for magnetic fields below about 60 kG, we can offer an explanation for the absence of hole oscillations in the reflectivity for the binary orientation. If the dependence of the hole relaxation time upon the magnetic field is roughly the same for the two orientations, then we would expect to see hole oscillations for the binary orientation at higher magnetic fields than for the bisectrix orientation, since the condition $\omega_c\tau \gg 1$ would be satisfied at lower field values for the bisectrix orientation. Furthermore, for the bisectrix orientation, larger fractional changes occur in the population of the magnetic subbands at a given value of the magnetic field, because of the lower cyclotron masses for the bisectrix orientations. An extension of the present experiments on the binary face to higher magnetic fields would provide a simple test of this hypothesis.

We can summarize our results with H parallel to the bisectrix axis as follows: (i) Reflectivity oscillations with the periodicities of both electrons and holes have been observed over the entire range of photon energies available from our laser. Furthermore, the amplitudes of these reflectivity oscillations are roughly independent of the photon energy. The hole oscillations have always been observed in connection with reflectivity minima, while the electron oscillations are associated either with minima or maxima, depending primarily upon the sample, but also upon the photon energy. The line-shape reversals which occur bear no relation to the plasma energy. The dHvA resonant fields are found to be independent of the photon energy. (ii) The amplitudes of the reflectivity oscillations associated with electrons are found to decrease gradually with the magnetic field, whereas those associated with holes exhibit a much stronger dependence upon the magnetic field. The strong decrease of the hole-reflectivity amplitudes with decreasing magnetic field suggests an explanation for the absence of hole oscillations for the binary orientation. The cyclotron effective mass for holes is heavier for the binary orientation than for the bisectrix orientation so that the condition $\omega_c\tau \gg 1$ is satisfied at lower magnetic fields for the bisectrix orientation.

C. Trigonal Orientation

The orientation for which the trigonal axis is parallel to the magnetic field is familiar from the calculations of Sec. II. At that point we remarked that, for the trigonal orientation, all of the hole ellipsoids and all of the electron ellipsoids are equivalent, so that the effective conductivity takes a particularly simple form, as we see in Eq. (11). For the trigonal orientation, Windmiller[3] finds the hole period to be 1.00×10^{-6} G^{-1} and the electron period to be about one-fourth as large. As we mentioned previously, we expect a single series of reflectivity oscillations with a period corresponding to that for holes.

In discussing the magnetoreflection data for the trigonal orientation, we wish to consider the three experimental traces of Fig. 9. From top to bottom, the traces were obtained at wavelengths of 12.913 μ

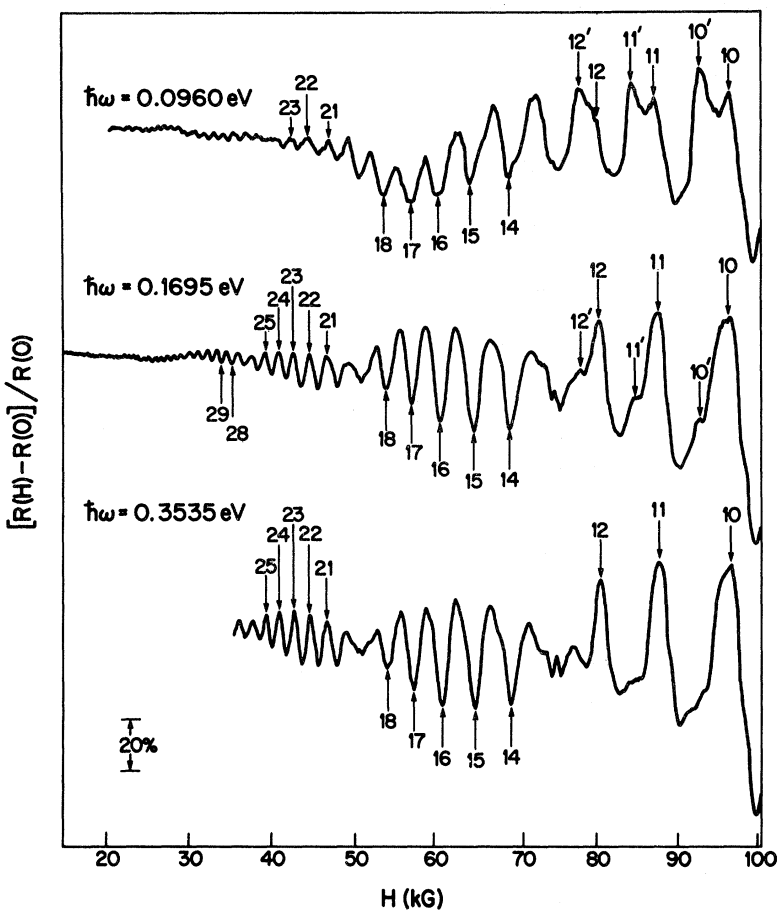

FIG. 9. Experimental magnetoreflection traces obtained at $\hbar\omega = 0.0960$, 0.1695, and 0.3535 eV. Sample temperature is $T = 2.1$ °K and $\vec{H}$ is parallel to the trigonal axis.

(= 0.0960 eV), 7.3147 μ (= 0.1695 eV), and 3.5070 μ (= 0.3535 eV); the sample temperature was about 2.1 °K in each case. The three traces of Fig. 9 illustrate nicely the two major discrepancies between the simple model and our experimental data, namely, the enormous amplitudes of the reflectivity oscillations and the weak dependence of the oscillatory amplitudes on photon energy. In the middle trace, for example, the amplitudes of the SdH oscillations grow from about 1% at 20 kG near where the $l = 50$ Landau level passes through the Fermi surface to about 90% at 95 kG near where the $l = 10$ Landau level passes through. We also find, for example, that the amplitude of the reflectivity oscillation associated with the passage of the $l = 10$ Landau level through the Fermi surface is roughly independent of the photon energy. In addition, these traces possess a number of features which are peculiar to the trigonal orientation. In order to study these features, it proves convenient to consider the traces individually.

In the middle trace ($\hbar\omega = 0.1695$ eV), we use the fact that the passage of a Landau level through the Fermi surface is associated with the narrow sharp portion of the oscillatory line shape, thereby identifying the reflectivity maxima labeled 10, 11, 12 with the dHvA resonant magnetic fields. From the magnetic field values for these maxima, we can make a quantum assignment. At slightly lower fields, the line shape indicates that the reflectivity minima are to be identified with the dHvA resonant fields and for these, also, we can make a quantum assignment. Using the period and phase obtained from a fit to the high-field data, we can make a quantum assignment for the reflectivity oscillations at lower magnetic fields. Then, using the reflectivity extrema labeled 10–25, we find $P = 0.993 \times 10^{-6}$ G^{-1}, which is in excellent agreement with Windmiller's result.[3] We also obtain $\Delta_H = 124$ G and $\Delta P/P = 0.23\%$, which supports both the quantum assignment and the contention that the Fermi level can be regarded as independent of the magnetic field in these experiments.

In a similar fashion, a quantum assignment can be made for the lowest trace of Fig. 9 ($\hbar\omega = 0.3535$ eV) and, from the reflectivity extrema labeled 10–25, we obtain $P = 0.996 \times 10^{-6}$ G^{-1} with $\Delta_H = 139G$ and $\Delta P/P = 0.23\%$. For the lower two traces of Fig. 9, the dHvA resonant fields associated with the passage of a particular Landau level through the

Fermi surface are the same as for the top trace to within the above-quoted values of Δ_H, indicating that the reflectivity oscillations are truly of SdH origin.

We also note that the line-shape reversals occur at the same magnetic fields for the two lower traces which were obtained at widely separated photon energies. This seems to rule out an explanation of the reversals in terms of a beating due to the superposition of SdH oscillations and interband Landau-level transitions. From experimental considerations, we can rule out beating effects due to crystal misalignment or the presence of two small crystallites. However, the relationship of the modulating envelope to the large reflectivity oscillations is illuminated by data obtained several days later from the sample which gave the traces of Fig. 9.[20] Although the sample had been maintained near the temperature of liquid nitrogen between the magnet runs, there was evidence of sample deterioration in the data obtained during the second magnet run. It was found that the amplitudes of the reflectivity oscillations fell off rapidly and the line-shape reversals at a single photon energy were absent.

We notice several important differences between the two lower traces of Fig. 9. The oscillatory-reflectivity amplitudes are larger in the lowest trace than in the middle trace, so that, in the lowest trace, they are nearly three orders of magnitude larger than the predictions of the simple theory of Sec. II. Furthermore, in the lowest trace, the high-field maxima have narrowed, while the side structures labeled 10′, 11′, 12′ in the middle trace have decreased in size. The noticeable dependence on photon energy of the amplitudes of the structures labeled 10′, 11′, 12′ in the middle trace is confirmed by our attempts to make a quantum assignment for the top trace of Fig. 9. If we were to make a fit to the reflectivity minima, we find that Δ_H and $\Delta P/P$ are several times larger than the corresponding values we obtain for the two lower traces and the value for the period differs by nearly 10% from the values of P obtained from the lower traces. These results suggest that a quantum assignment based on the reflectivity minima of the top trace is incorrect. Using, instead, the well-established frequency independence of the dHvA resonant fields to generate a quantum assignment, we obtain the assignment indicated in the top trace of Fig. 9. Making a fit to the reflectivity extrema labeled 10–23 we obtain $P = 0.998 \times 10^{-6}$ G^{-1} and values for Δ_H and $\Delta P/P$ which agree well with those obtained for the two lower traces. This quantum assignment involves several line-shape reversals in the top trace and suggests that the amplitudes of the structures labeled 10′–12′ depend strongly upon the photon energy. Although the line-shape reversals are not the most obvious feature of the upper trace, this quantum assignment preserves the frequency independence of the dHvA resonant fields and gives a value for the period which is consistent with the lower traces.

The doublet structure of the high-field maxima of the upper trace suggests the spin splitting of the Landau levels. Using the cyclotron-mass data of Datars and Vanderkooy[18] to compute the g factors associated with this splitting, reasonable agreement is reached with the g factor determined by Datars[28] for holes for the trigonal orientation. Thus, we have a situation similar to that which we encountered in connection with the traces of Fig. 6 for the binary orientation; there is a doublet structure in the high-field reflectivity extrema which may be associated with the spin splitting of the Landau levels. Furthermore, the amplitude of one member of the doublet exhibits a strong dependence upon photon energy, while the amplitude of the other member is relatively independent of the photon energy. However, other experimental traces from samples of poorer quality failed to exhibit the doublet structure at high fields.[20] An extension of the present experiments to still higher magnetic fields should permit a more accurate determination of these splittings to be made and should allow observations of this structure on samples of poorer quality.

In addition to several line-shape reversals on a single experimental trace (magnetic-field-dependent reversals), we have also observed the passage of a Landau level through the Fermi surface to be associated with either minima or maxima in the reflectivity, depending upon the photon energy. This occurs at low temperatures (~2 °K), on poorer samples, where there are no magnetic-field-dependent line-shape reversals, and the reversals occur at a photon energy which bears no relation to the plasma energy. Furthermore, at slightly higher temperatures (~4 °K), the dHvA resonant fields are all found to be associated with either reflectivity minima or maxima, independent of the photon energy.

Finally, we mention that the amplitudes of the reflectivity oscillations were found to be independent of the temperature below 2.1 °K. A noticeable change in the amplitudes was observed when the temperature was lowered from 4.2 to 2.1 °K and, in some cases, this change amounted to an increase in the amplitudes by more than a factor of 2. The experimental difficulties involved in working in this temperature region make our measurements uncertain and prevented a more quantitative study of the temperature dependence of the SdH amplitudes from being made.

V. DISCUSSION

We have found that the results of the laser mag-

netoreflection experiments differ in two major respects from the predictions of the simple theory of Sec. II. First, for magnetic fields near 100 kG, fractional changes in the reflectivity approaching 100% are observed when a Landau level passes through the Fermi surface. Second, the large fractional changes in the reflectivity are observed over the entire range of photon energies available from our laser, and the reflectivity amplitudes are found to be roughly independent of the photon energy. On the other hand, we find that the periods associated with the large reflectivity oscillations agree very well with the periods measured in dHvA experiments[3] for the corresponding orientations of the magnetic field with respect to the crystallographic axes. Furthermore, the dHvA resonant fields associated with the reflectivity extrema are found to be independent of the photon energy, indicating that the reflectivity oscillations are connected with a dHvA-like mechanism in the optical conductivity.

The analysis of the dc SdH experiments of Rao *et al.*[5] and Long *et al.*[6] indicates that we might begin to extend our simple theory by considering the effect of the magnetic field on the scattering processes. To obtain a physical feeling for how the scattering might be affected by the magnetic field, we may think of a magnetic-energy-level diagram where the energy levels associated with the carrier pockets are plotted as a function of momentum along the magnetic field. The Landau level spacing is $\hbar\omega_c$ and conduction is due to the carriers in a small band of width kT about the Fermi energy. As the magnetic field increases, the carriers in the Landau level closest to the Fermi surface have smaller and smaller momenta along the magnetic field. Therefore, when a carrier in this level is scattered, it will not have enough momentum to carry it away from the scatterer, but it will be scattered repeatedly, becoming, in effect, bound to the scatterer. Thus, it will contribute little to conduction and there will be a decrease in the conductivity.[29] If we think in terms of the magnetic field dependence of the relaxation time, this physical picture suggests that the relaxation time should exhibit oscillations which are periodic in the inverse magnetic field. This effect should become very important as the number of Landau levels below the Fermi surface becomes small.

If we consider the magnetic field dependence of the scattering, the problem of calculating the intraband conductivity becomes considerably more difficult since terms like $(\omega-\omega_c+i/\tau)^{-1}$ can no longer be removed from the summation of Eq. (1). Further complications arise because the effects of the electric field on the scattering must be included in a correct quantum-mechanical calculation of the conductivity, as recent calculations of the dc conductivity have shown.[30–32] Furthermore, the simplifications which occur in the calculation of the dc conductivity would not obtain for electric fields of finite frequencies.[30,32] Recently an approach to the problem of determining the magnetoconductivity for electric fields of arbitrary frequency has been given by Argyres,[33] for scattering by acoustic phonons, and by Argyres and Kirkpatrick,[34] for scattering by ionized impurities. These authors recognize that the usual assumptions, whereby the system relaxes to a state of thermal equilibrium appropriate to the instantaneous value of the total Hamiltonian,[35] cannot be correct for optical frequencies. Thus, they find that the interference between the electric field and the scattering interactions is frequency dependent and retains a rather complicated form. In both of these papers, solutions to the kinetic equations for the one-electron density operator are found. However, these solutions are non-Markovian in form and are, therefore, not easily applicable to an experimental situation.

There has, however, been one attempt to apply the results of more rigorous calculations of the conductivity to practical situations. This is the attempt of Mase[36] to extend the results of a calculation by Argyres[37] to high frequencies. Considering the effects of both the magnetic and the static electric fields on scattering, Argyres[35] finds that, for isotropic scattering mechanisms, the solution of the transport equation may be found for arbitrary values of $\omega_c\tau$. Furthermore, treating scattering only in the first Born approximation, Argyres finds that the scattering frequency is proportional to the density of states in the magnetic field. This is the kind of result we might expect from the simple physical picture which we discussed above. Mase[36] extended the results of Argyres by making a slight modification in the form of the time development of the density matrix. Using the frequency-independent relaxation time of Argyres, Mase obtains an expression for the intraband contribution to the dielectric constant which leads to large reflectivity oscillations near the plasma edge. However, Mase's results indicate that the amplitudes of the reflectivity oscillations should decrease rapidly with photon energy, which is in disagreement with our experimental results. Furthermore, Mase's results also predict a lineshape reversal at the plasma edge, which we do not observe. These discrepancies between our experimental results and the predictions of Mase's more rigorous formulation of the intraband conductivity indicate that intraband effects will not be sufficient to explain our data, unless the frequency dependence of the scattering leads to drastic changes in the form of the optical conductivity. However, we do not expect this to be the case because Eq. (1) has been used to interpret other mag-

netoreflection experiments.[13,14]

Since intraband contributions to the dielectric constant cannot be important at high photon energies, it is then most obvious to consider the interband conductivity, which can make a substantial contribution to the dielectric constant for photon energies exceeding a band gap. If we consider our experimental data, together with our previous discussions of the intraband contribution to the dielectric constant, we can get an idea of what form this interband contribution must take. We know that the oscillatory reflectivity line shape associated with an intraband contribution must undergo a reversal at the plasma edge, as the real part of the dielectric constant changes sign. Thus, we require a substantial dHvA-like interband contribution slightly above the plasma edge so that the dHvA resonant fields are always associated with either maxima or minima in the reflectivity depending upon the sample, for photon energies above and below $\hbar\omega_p$. Furthermore, we require a large dHvA-like contribution at high photon energies, well above the plasma edge, to give the large dHvA-like oscillations in the reflectivity at those photon energies.

In fact, we know that in antimony there are important interband contributions to the dielectric constant for photon energies near the plasma edge as well as for energies above the plasma edge. Interband transitions associated with a gap of 0.10 eV have been observed,[38] which have been identified with a band gap at the Q point.[39] This Q-point band gap has been found to be very important for determining the optical properties in the neighborhood of and above the plasma edge. In addition, there is another series of interband transitions, associated with a band gap of 0.14 eV, which has been observed in the magnetoreflection spectrum of antimony.[38] Furthermore, from Nanney's optical data at zero magnetic field,[23] we know that there is a broad strong contribution to the reflectivity from an absorption edge around 2.9 μ (0.43 eV). This band edge is probably associated with interband transitions at the carrier pockets and the breadth of the absorption minimum[23] indicates that the contributions to the dielectric constant from this band edge are substantial at photon energies below 0.43 eV.

We must now consider how a dHvA-like interband contribution may arise. For energies below the energy for which interband transitions are allowed, the interband contribution is primarily dispersive, that is, the primary contribution is to ϵ_1. This contribution extends below the energy gap, as the Kramers-Kronig relations require, and the width and amplitude of the dispersive contribution depend critically upon the interband relaxation time. Now the interband relaxation time is a measure of the time necessary for an electron which has been excited to a conduction-band state to return to thermal equilibrium at the Fermi level and this may be accomplished either through radiative or nonradiative processes. Therefore, since the dispersive contribution to the dielectric constant may depend strongly upon the scattering of the carriers, this contribution may also exhibit the same kind of magnetic field dependence as the scattering time. The dependence of the interband relaxation time on the magnetic field and photon energy has not been studied in any detail, in contrast to the situation for the intraband relaxation time.[33] However, since these interband effects may give us a mechanism for extending the frequency response of the relaxation effects we have mentioned, these interband effects should be given further consideration.

However, the quantitative application to antimony of the results of a theoretical study of the magnetic field and photon-energy dependence of the interband relaxation time would encounter an additional difficulty, namely, the lack of an adequate band model for the energy range $0.10 < \hbar\omega < 0.50$ eV. There are several closely related reasons for this. Not only does the pseudopotential band model of Falicov and Lin[15] not include the spin-orbit interaction, which is essential for this energy range, but also the results of the interband-magnetoreflection experiments[38] have not yet been incorporated into the band model. Furthermore, the only experimental information on the band gap giving rise to the absorption minimum at 2.9 μ comes from the zero-field experiments of Nanney.[23]

This lack of information is sorely felt because there is another mechanism which may be applicable to our experimental data for a considerably smaller theoretical effort than those mentioned above. Looking at the Faraday rotation of n-type PbS, Mitchell *et al.*[40] observed extremely large dHvA-like oscillations in the interband contribution. The amplitudes of these oscillations were several orders of magnitude larger than those which could be expected from carrier-density oscillations.[41] Furthermore, for photon energies below the Burstein-Moss energy, the periods of the oscillations were found to be independent of the photon energy but dependent upon the carrier concentration. The oscillations were periodic in the inverse magnetic field and, from the periods, the carrier concentrations were determined and found to agree with the results of Hall measurements to within 20%. Mitchell *et al.*[40] interpreted their experiments in terms of a contribution to the off-diagonal elements of the interband conductivity due to a difference in population of the two Kramers's states of the populated band. For energies below the Burstein-Moss energy, this mechanism gives rise to the large dHvA-like oscillations in the Faraday rotation whose amplitudes are relatively indepen-

dent of the photon energy.[41] There are many interesting similarities between the experimental results of Mitchell *et al.* and the results of our laser-magnetoreflection experiments. It is extremely suggestive of a connection between the two that the most probable locations for the band gap associated with the absorption edge at 2.9 μ are the locations of the carrier pockets. However, an application of this mechanism to our data requires information about the matrix elements, g factors, and effective masses associated with this band gap and this information is not presently available. A pseudopotential calculation which includes the effects of the spin-orbit interaction and which is being constructed to fit the interband-magnetoreflection data is currently in progress.[42]

ACKNOWLEDGMENTS

We would like to express our thanks to R. W. Brodersen, Dr. V. G. Veselago, and Dr. D. L. Mitchell for stimulating discussions. We are especially appreciative of the constant help with the experimental work provided by Dr. S. Iwasa and the encouragement extended by Professor A. Javan.

---

*Paper based on a thesis submitted by one of the authors (F.P.M.) in partial fulfillment of the Ph.D. degree in the Physics Department, Massachusetts Institute of Technology, Cambridge, Mass. (1971).

†Work supported in part by the Advanced Research Projects Agency, Contract No. SD-90, by NASA Washington Contract No. NGL-22-009-012, by the Air Force Cambridge Research Laboratory Contract No. F-19-(628)-68-C-0204, by the Department of the Air Force, and by the Air Force Office of Scientific Research.

‡Present address: University of São Paulo, São Paulo, Brazil.

§Visiting scientists, Francis Bitter National Magnet Laboratory, Massachusetts Institute of Technology, Cambridge, Mass., now supported by the National Science Foundation.

[1]D. Shoenberg, Phil. Trans. Roy. Soc. London A245, 1 (1952).

[2]Y. Saito, J. Phys. Soc. Japan 18, 452 (1963); Y. Ishizawa and S. Tanuma, *ibid.* 20, 1278 (1965); N. B. Brandt, N. Ya. Minina, and Chu Chen-Kang, Zh. Eksperim. i Teor. Fiz. 51, 108 (1966) [Sov. Phys. JETP 24, 73 (1967)]; J. B. Ketterson and L. R. Windmiller, Phys. Rev. B 1, 463 (1970).

[3]L. R. Windmiller, Phys. Rev. 149, 472 (1966).

[4]J. Ketterson and Y. Eckstein, Phys. Rev. 132, 1885 (1963); L. S. Lerner and P. C. Eastman, Can. J. Phys. 41, 1523 (1963); N. B. Brandt, E. A. Svistova, and T. V. Gorskaya, Zh. Eksperim. i Teor. Fiz. 53, 1274 (1967) [Sov. Phys. JETP 26, 745 (1968)].

[5]G. N. Rao, N. H. Zebouni, C. G. Grenier, and J. M. Reynolds, Phys. Rev. 133, A141 (1964).

[6]J. R. Long, C. G. Grenier, and J. M. Reynolds, Phys. Rev. 140, A187 (1965).

[7]Y. Eckstein, Phys. Rev. 129, 12 (1963); J. B. Ketterson, *ibid.* 129, 18 (1963); L. Eriksson, O. Beckman, and S. Hornfeldt, J. Phys. Chem. Solids 25, 1339 (1964).

[8]B. McCombe and G. Seidel, Phys. Rev. 155, 633 (1967).

[9]S. Noguchi and S. Tanuma, Phys. Letters 24A, 710 (1967).

[10]M. S. Dresselhaus and J. G. Mavroides, Solid State Commun. 2, 297 (1964).

[11]P. N. Argyres, Phys. Rev. 109, 1115 (1958).

[12]P. A. Wolff, J. Phys. Chem. Solids 25, 1057 (1964).

[13]M. S. Maltz, Ph.D. dissertation (Massachusetts Institute of Technology, 1968) (unpublished).

[14]P. R. Schroeder, Ph. D. dissertation (Massachusetts Institute of Technology, 1969) (unpublished).

[15]L. M. Falicov and P. J. Lin, Phys. Rev. 141, 562 (1966).

[16]A. H. Kahn and R. P. R. Frederikse, in *Solid State Physics*, Vol. 9, edited by F. Seitz and D. Turnbull (Academic, New York, 1959), p. 257.

[17]B. Lax, K. J. Button, H. J. Zeiger, and L. M. Roth, Phys. Rev. 102, 715 (1956).

[18]W. R. Datars and J. Vanderkooy, IBM J. Res. Develop. 8, 247 (1964).

[19]L. Onsager, Phil. Mag. 43, 1006 (1952).

[20]F. P. Missell, Ph. D. Dissertation (Massachusetts Institute of Technology, 1971) (unpublished).

[21]It is convenient to define the principal mirror plane as the one perpendicular to the binary axis of the sample. The other two mirror planes are referred to as the nonprincipal ones. Then the principal and nonprincipal carrier ellipsoids are defined as the ellipsoids whose centers lie in the principal and nonprincipal mirror planes, respectively.

[22]Y. Beers, *Introduction to the Theory of Error* (Addison-Wesley, Reading, Mass., 1957), pp. 38–43.

[23]C. Nanney, Phys. Rev. 129, 109 (1963).

[24]I. M. Lifshitz and L. M. Kosevitch, Zh. Eksperim. i Teor. Fiz. 33, 88 (1957) [Sov. Phys. JETP 6, 67 (1958)].

[25]G. E. Zil'berman, Zh. Eksperim. i Teor. Fiz. 29, 762 (1955) [Sov. Phys. JETP 2, 650 (1956)].

[26]M. Greenbaum, Ph.D. dissertation, p. 48 (Massachusetts Institute of Technology, 1968) (unpublished).

[27]G. E. Smith, L. C. Hebel, and S. J. Buchsbaum, Phys. Rev. 129, 154 (1963).

[28]W. R. Datars, Phys. Rev. 126, 975 (1962).

[29]R. Kubo, S. J. Miyake, and N. Hashitsume, in *Solid State Physics*, Vol. 17, edited by F. Seitz and D. Turnbull (Academic, New York, 1966), p. 269.

[30]P. N. Argyres and L. M. Roth, J. Phys. Chem. Solids 12, 89 (1959).

[31]E. N. Adams and T. D. Holstein, J. Phys. Chem. Solids 10, 254 (1959).

[32]R. Kubo, H. Hasegawa, and N. Hashitsume, J. Phys. Soc. Japan 14, 56 (1959).

[33]P. N. Argyres, Phys. Rev. 132, 1527 (1963).

[34]P. N. Argyres and E. S. Kirkpatrick, Ann. Phys. (N. Y.) 42, 513 (1967).

[35]R. Karplus and J. Schwinger, Phys. Rev. 115, 1342 (1959).

[36]S. Mase, J. Phys. Soc. Japan 21, 243 (1966).

[37]P. N. Argyres, Phys. Rev. 117, 315 (1960).

[38]M. S. Dresselhaus and J. G. Mavroides, Phys. Rev. Letters 14, 259 (1965).

[39]M. S. Dresselhaus, in *The Physics of Semimetals and Narrow Gap Semiconductors*, edited by D. L. Carter and R. T. Bate (Pergamon, New York, 1971), p. 3.

[40]D. L. Mitchell, E. D. Palik, and R. F. Wallis, J. Phys. Soc. Japan Suppl. 21, 197 (1966).

[41]D. L. Mitchell (private communication).

[42]R. W. Brodersen (private communication).

PHYSICAL REVIEW B VOLUME 5, NUMBER 4 15 FEBRUARY 1972

Contribution of Defect Dragging to Dislocation Damping. I. Theory*

H. M. Simpson† and A. Sosin
University of Utah, Salt Lake City, Utah 84112

(Received 26 August 1971)

The contribution of dragging of point defects attached to dislocation lines, to dislocation damping, to elastic modulus, and to logarithmic decrement, is developed. It is shown that the dragging leads to an initial increase in decrement in a suitable frequency range, determined by other related parameters: dislocation loop length, line tension, and damping constants. The theory predicts a dependence on frequency of ω^{-1}, in contrast to the Koehler-Granato-Lücke (KGL) frequency dependence of ω, explaining the failure of previous experiments to confirm the KGL theory. In a similar manner, the generally accepted dependences on point-defect density are shown to be incorrect at lower frequencies, below a few kHz in copper. For example, it is shown that the dislocation decrement should be proportional to the two-thirds power of the modulus defect, rather than proportional to the square of the modulus defect as previously expected, at large point-defect densities on dislocation lines.

I. GENERAL INTRODUCTION

Some thirty years have passed since Read suggested that dislocations contribute notably to the internal friction of metals.[1] Since then, several mechanisms for this contribution have been proposed and developed.[2,3] The most successful of these, the one most commonly used for interpretations of experimental observations, was initiated by Koehler in 1950.[4] The model was shortly thereafter developed in more detail by Granato and Lücke.[5] Henceforth we shall refer to this as the KGL theory of internal friction.

The KGL model is a string model for a dislocation. In this model the dislocation is endowed with all the attributes of a string so that the mathematical formalism begins with a string equation

$$A\frac{\partial^2 y}{\partial t^2}+B\frac{\partial y}{\partial t}-C\frac{\partial^2 y}{\partial x^2}=\sigma_0 b e^{-i\omega t}\ . \tag{1}$$

In Eq. (1), A is the effective mass per unit length of dislocation, B is a viscous damping constant, C is the effective line tension of the dislocation, assumed constant, b is the magnitude of the Burger's vector of the dislocation, σ_0 is the amplitude of the applied harmonic stress of angular frequency ω, y is the displacement of an elemental portion of the string at a distance x from one end of the string, and t is time. $A=\pi\rho b^2$, where ρ is the mass density of the material. Each term in Eq. (1) is a force per unit length of dislocation.

The problem is formulated for a dislocation of length l at zero stress so that the boundary conditions on Eq. (1) are

$$y(0,t)=y(l,t)=0. \tag{2}$$

In all of this article we shall be concerned with frequencies sufficiently low (lower than about 10 kHz), so that the inertial term (the first term in the string equation) may be neglected. This may be verified by inserting generally accepted values of B, greater than 5×10^{-5} dyne sec cm^{-2}, and dislocation velocities, limited by (and well below) the speed of sound, in the first two terms of Eq. (1).

Having disposed of the first term in Eq. (1), one may still question the appropriateness of each of the remaining terms: (i) $B\,\partial y/\partial t$. This term represents the viscous damping of dislocation motion, under stress. Since actual dislocation motion involves the creation and motion of kinks, the mounting of Peierl's barriers, etc., the concept of simple viscous motion is an idealization, but the work of Trott and Birnbaum shows that these complexities are reasonably well averaged over in a string model.[6] Furthermore, Leibfried has calculated B in a model of phonon scattering at dislocations, lending further credence to this term.[7] We shall continue to adopt a viscous-force term but with reservations. As developed later, we believe that impurity effects have been underestimated and, concomitantly, the actual dislocation-line damping, overestimated. Also, the possible validity of other frictional terms should be considered. The classical case of constant sliding friction may be important, for example. (ii) $C\,\partial^2 y/\partial x^2$. This